Supplemental Material

Sedimentary Inputs to the Nankai Subduction Zone:

The Importance of Dispersed Ash

Rachel P. Scudder, Richard W. Murray, Steffen Kutterolf, Julie Schindlbeck, Michael B. Underwood, Kuo-Lung Wang

Sources of volcanic ash to the Nankai region

This section of the Supplemental Material is related to Section 2 of the main text.

Shikoku Basin Paleogeography

The Shikoku Basin formed between 30 and 15 Ma due to back-arc rifting and seafloor spreading in the eastern part of the Philippine Sea plate (Taylor, 1992; Sdrolias et al., 2004; Pickering et al., 2013). Since its formation, the history of the Shikoku Basin has been complex (Figure S1). During the Neogene alone it is thought that six main tectonic events occurred (Kano et al., 1991; Taira, 2001). First rifting of the paleo–Izu-Bonin Arc and opening of the Shikoku Basin via seafloor spreading has been interpreted as occurring from ~25 to ~15 Ma. Following or coincident with the rifting of the paleo-Izu-Bonin Arc, rifting of the paleo–Honshu continental arc and spreading of the Japan Sea basin is believed to occur from ~22 to ~15 Ma. The rifting caused Japan to break away from Eurasia, and SW Japan (Honshu) to rotate clockwise ~45º as it drifted south (Kimura et al., 2005, Pickering et al., 2013). From ~17 to ~12 Ma the SW Honshu arc exhibited widespread, near-trench igneous activity. At ~15 Ma the initiation of subduction of the Philippine Sea plate and collision of the Izu-Bonin Arc against the SW Honshu Arc is thought to have occurred, and was followed by a major episode of

subduction of the Philippine Sea plate beginning at 8 Ma. Additionally, there was collision with a portion of the Kurile fore-arc mountain building beginning at ~15 Ma (Kano et al., 1991; Taira, 2001; Pickering et al., 2013).

Further complexities result from changes in subduction in the region. On the Kyushu arc, Pacific plate subduction dominated prior to 15 Ma however, from 15 to 6 Ma, changes in relative plate motions caused the triple junction to shift between the Pacific plate, Philippine Sea plate, and southwest Japan northward causing the Philippine Sea plate to be subducted beneath Kyushu (Mahony et al., 2011). From ~10-6 Ma there is an observed lack of subduction-related volcanism on Kyushu which has been credited to shallow subduction of young Shikoku Basin lithosphere (Mahony et al., 2011; Pickering et al., 2013). By ~6-5 Ma Philippine Sea plate motion changes resulted in rapid, nearly trench normal, subduction beneath Kyushu. The model of Mahony et al. (2011) also calls for the initial collision between the Izu-Bonin Arc with the SW Japan (Honshu) Arc to occur at ~8-6 Ma, much later than the ~15 Ma age which has been widely accepted (e.g., Tamura et al., 2010; Tani et al., 2010; Yamazaki et al., 2010). Additionally, lateral motion and collision of the Izu-Bonin and Honshu Arcs is modeled for the time between ~10 and ~5 Ma (Hall, 2002; 2012; Pickering et al., 2013). Evidence does exist for collision and accretion of crustal material associated with Mio-Pliocene sedimentary basins forming in the Izu-Honshu collision zone as far back as 17–15 Ma (e.g., Soh et al., 1991; Tani et al., 2010) and Pickering et al. (2013) note that the present northern part of the Izu-Bonin Arc contains ~50 Ma arc crust and suggest that it may include the remnants of the ~17–15 Ma ridge collision.

Arc Paleovolcanism

There is evidence of volcanism on Kyushu associated with mid Miocene subduction that is recognized today in a band of felsic plutonic rocks (Figure S1). These are assumed to represent the igneous activity associated with the arc volcanism occurring to the northwest from ~15-10 Ma (Kimura et al. 2015). The band of plutons trends NE-SW across the central volcanic region indicating a northwestward subduction direction, similar to what is seen today. These plutons form part of much more widespread igneous activity which took place within the SW Japan forearc between 17-13 Ma (Kano et al., 1991). This subduction led to the formation of high magnesium andesites in SW Japan (Suzuki and Tatsumi, 2006). At ~15 Ma, offshore Kyushu, the final stages of Sea of Japan opening led to rifting of the western margin of NE Honshu (Yamaji, 1990). This rifting was accompanied by eruption of a large volume of submarine volcanic rocks (Taira, 2001).

Caldera forming felsic volcanism in the NE Japan arc started about 13 Ma in response to enhanced subduction of the Pacific plate beneath the continental crust of Japan (Sato, 1994). Along the main part of the arc (NE Honshu), caldera volcanoes cluster at every 40-80 km forming six volcanic centers each comprising 3 to >10 calderas (Yamamoto, 2009). Most of the caldera forming eruptions took place during the initial uplift in the Late Miocene to Pliocene (Acocella et al., 2008). During the last 15 m.y., the position of the IBM migrated from its position off southern Honshu (15 Ma) towards its northernmost location north of the Boso Peninsula (central Honshu, 2Ma) (Mahony, 2011). Due to this migration, the influence of volcanism from the IBM on the Nankai Trough area varies with time showing for example a significant increase of explosive

volcanism from the Izu-Bonin region 17 Ma and 2 Ma ago (Taylor 1992, Stern et al. 2003).

The volcanoes of the Quaternary Honshu arc are well known for large-scale explosive volcanism (Machida, 1999). Whereas the northern part of Honshu is characterized by caldera forming eruption, the central to western volcanic centers on Honshu and the Izu-Bonin-Mariana Arc are characterized by stratovolcanoes that only in part are connected to calderas (Machida, 1999). From Quaternary times, 16 calderas are known on Honshu with the majority in central and northern Honshu. Machida et al. (1999; 2002) established a tephrostratigraphic framework of 26 Quaternary widespread tephra layers in and around Japan, including five tephras originated from Honshu (Machida and Arai, 2003). Quaternary explosive volcanism at the northern Izu-Bonin arc is associated with eight submarine calderas and eleven island volcanoes and shows a bimodal composition with rhyolitic dominated calderas and basaltic dominated island volcanoes (e.g. Tamura and Tatsumi, 2002).

Assessment of Multivariate Statistical Analyses:

This section of the Supplemental Material is related to Section 5 of the main text. In order to ensure that we have obtained statistically robust results, our group takes an approach to dealing with some of the limitations for both factor analysis (QFA) and the constrained least squares (CLS) multiple linear regression that is strategically built around performing dozens to hundreds of statistical runs per dataset to assess sensitivity of, and variability in, the results. Previously, this approach was very labor-intensive, performing the numerous statistical runs manually. Dunlea and Murray (2015), however,

provide MATLAB codes that reduce the time and labor involved in testing and determining a robust and stable CLS model. The newly optimized codes allow the user to input multiple sources at one time, while the program then runs all possible combinations of the sources based on the number of end-members defined by the QFA analyses (that is all combinations of 3 sources, all combinations of 4 sources, etc…). The program then provides, as output, the top ten combinations of end-members with the highest r-values (coefficients of determination). These results are presented in Table S9. The results were evaluated for accuracy and to ensure that they were geologically reasonable.

The relative strength of the different multiple linear regression models was assessed through several methods. First, a study of the correlation coefficients (r-values) allowed for comparison of the predictive capability of the different models. The model code places a high priority on maximizing the r-values (and minimizing residuals), even if the consequence of doing so is to generate a geologically unreasonable abundance of a known end member. As a result, Al and Ti, as major elements, have "perfect" ($r = 1$) or near perfect r-values in all models. Therefore, we focused on identifying end-member combinations with a balance of as high as possible r-values for the trace and REEs. Additionally, sometimes the model result would be geologically unreasonable in terms of presenting too high an abundance (e.g., loess = 90 wt. %), which would contradict the visual observations (e.g., smear slides, sedimentological observations) or insight from other geochemical approaches (e.g., normative calculations, mass balances). Thus, the selected models present the best results in terms of coefficients of determination as well as being geologically consistent with the independent observations.

Given that Sites C0011 and C0012 have uniformly high r-values (i.e., very few r-values <0.10, very few negative values) the selection is admittedly somewhat subjective. However, considering the combined dataset and Site C0012, it is clear that none of the combinations with Izu-Bonin Front Arc material are successful as based on the above criteria. In particular, the r-values for Cr are very low in these models, therefore they are excluded from the averaged models. For Site C0011 the r-values are less clear, however at this site the models containing Izu-Bonin Front Arc material are not geologically reasonable and therefore these models are excluded from the average.

Considering Sites C0011 and C0012 as Separate Datasets

This section of the Supplemental Material is related to Section 6 of the main text. Overall the combined models from Site C0011 and C0012 provide a good record of the overall input into the Nankai Subduction Zone. Performing statistical analysis on the Sites C0011 and C0012 individually can allow us to further characterize the detailed sources to the sediment in this region. At Site C0011, the CLS multiple linear regression identifies that the aluminosilicate component of the bulk sediment is best described with the four sources being compositionally modeled by a mixture of Asian Dust, a Rhyolitic Ash, Dacitic Ash, and Kyushu Ash (Figure 3, Table S7). Consistent with the combined model for Site C0011 (Section 6.2 of the main text) we arrived at this set of sources by averaging from the top ten models. Here we averaged six of the top ten models excluding four models with a significant IBFA component as the sedimentological data indicates predominately felsic material (Table S6). For the "Asian Dust" component, of the six models four utilize Chinese Loess and two contain PAAS. The "Dacitic Ash" in this case

consists of four models containing Dacite from the Honshu Arc (HD) while the other two models contain Dacite from the Izu-Bonin Arc. The "Kyushyu Ash" component at Site C0011 is split evenly between Dacite and Andesite from the Kyushu Arc.

As with the combined model discussed in Section 6.2, the model that best explains the composition of the sediment at Site C0011 includes an end-member based on the chemistry of the discrete ash layers (Tables S2A and S3A). We therefore interpret that a portion, or even all, of the "Rhyolitic Ash" dispersed ash component is the result of ash that was transported through the atmosphere. Analogously, because none of the end-members that make up the Dacitic or Kyushu Ash components appear in discrete layers, we interpret that they are more likely to be erosional or transported by density currents (e.g. Schindlbeck et al. 2013, Kutterolf et al. 2014), although a portion could be transported through the atmosphere as well. These results are consistent with the modeling based on grouping the two separate sites into one dataset (Section 6.2).

Of the top ten CLS models at Site C0012, we excluded three based on the significant presence of IBFA (Section 6.2.2). At this site the "Asian Dust" is averaged from six models containing Chinese Loess and one model with PAAS. The models for "Rhyolitic Ash" and "Dacitic Ash" are less clear-cut than their equivalents at Site C0011. Here, the "Rhyolitic Ash" is an average of two models containing the rhyolitic ash layer from Nankai, two models with Andesite from the Arc, two models with Rhyolite from the Izu-Bonin Arc, and one model containing the dacitic ash layer from Nankai. The "Dacitic Ash" is of mixed composition, consisting of an average of two models containing Dacite from the Izu-Bonin Arc, two models containing Andesite from the Izu-Bonin Arc, one model containing Rhyolite from the Izu-Bonin Arc, and two models containing Rhyolite

from the Honshu Arc. While the "Kyushu Arc" dispersed component is averaged from three distinct models containing Dacite or Andesite from the Kyushu Arc, and one model containing Andesite from the Izu-Bonin Arc. Kyushu Ash

Overall, the results from the individual modeling of Sites C0011 and C0012 are consistent with other studies of the tuffaceous and volcaniclastic sandstones, which outline mixed origins for the volcanic material from both the Izu-Bonin and Honshu Arcs (e.g., Kutterolf et al., 2014; Pickering et al., 2013; Schindlbeck et al., 2013). Our results are inconsistent with the findings of Saitoh et al. (2015) who, through the application of Sr, Nd, and Pd isotopes, suggested that at Site C0011 the sediment was mixed from the southwest Japan arc and from the area around the East China Sea. The differences in our findings may reflect methodological differences or a lack of data from the East China Sea region for inputs into our model.

The Total Amount of Dispersed Ash; Mass Balance Comparisons

This section of the Supplemental Material is related to Section 8 of the main text. For each site we calculated the cumulative mass (g) of ash found in the discrete ash layers in a 1 cm x 1 cm vertical column of sediment, and compared that to the cumulative mass of dispersed ash (and altered clay products) in the same 1 cm^2 vertical sediment column. For this 1 cm^2 column of sediment, these calculations are as follows:

(1) Mass (g) of *discrete* ash layers, per cm^2 =

Total thickness of ash layers (cm) x Average density of ash layers (g/cm^3).

And,

(2) Mass (g) of *dispersed* ash, per cm^2 =

(Total sediment thickness (cm) - Sum of discrete layer thicknesses (cm)) x DBD of the bulk sediment (g/cm^3) x (Fraction of dispersed ash in bulk sediment, in units of wt. % / 100).

For Site C0011, the total sediment thickness for which these calculations were performed was from the seafloor to the base of Hole C0011B, just below the Unit IV/V boundary (~878 m of sediment), and for Site C0012 the total thickness for which these calculations were performed was from the seafloor to the base of Unit V in Hole C0012A (528 m of sediment).

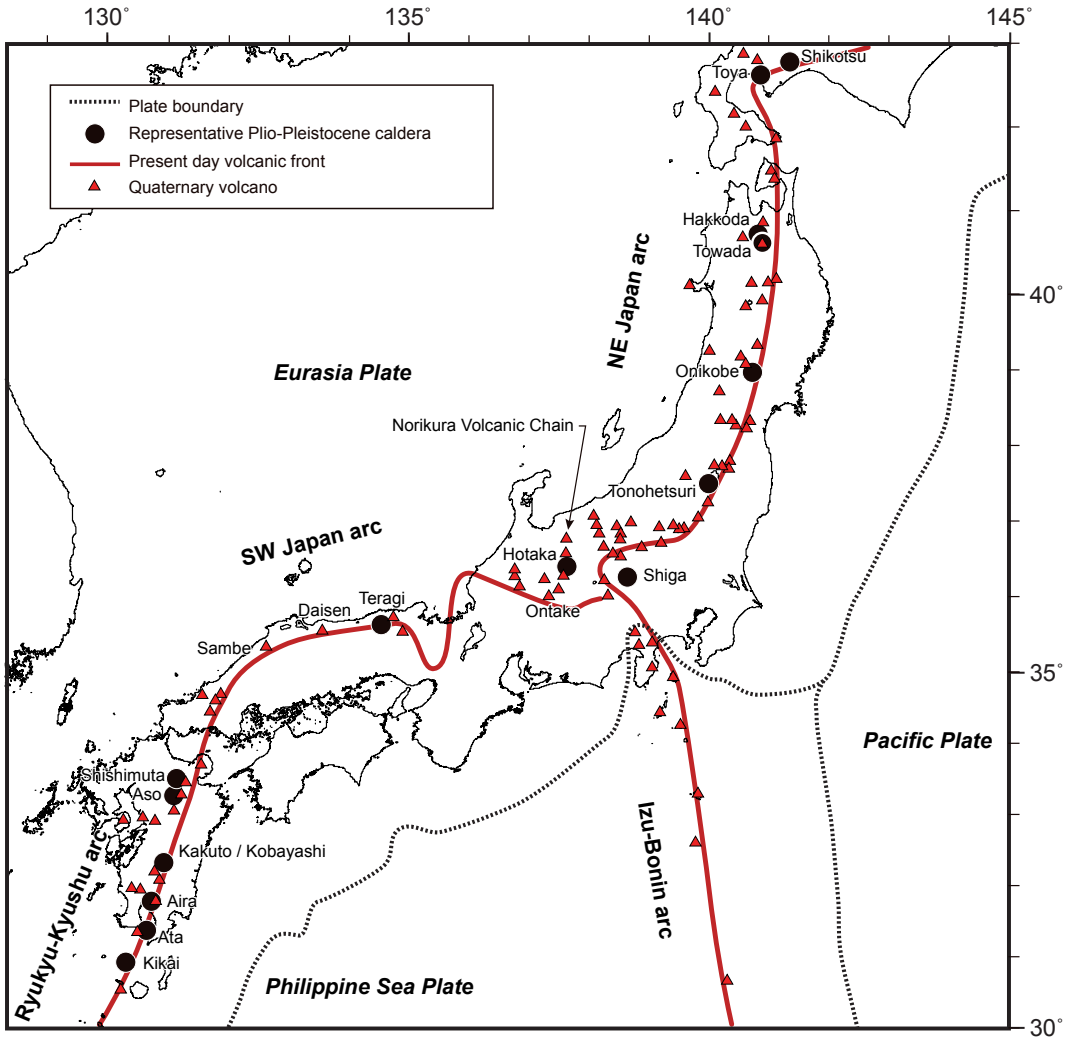

Fig. S1: Tectonic map of the Japanese Islands and locations of Quaternary volcanoes and representative late Cenozoic calderas modified after Kimura et al. (2015). The present day volcanic front is given in red.

References Cited

Acocella, V., Yoshida, T., Yamada, R., Funiciello, F., 2008.Structural control on late Miocene to Quaternary volcanism in the NE Honshu arc, Japan, Tectonics, 27: TC5008, http://dx.doi.org/10.1029/2008TC002296

Dunlea A. G. and Murray R. W., 2015, Optimization of end-members used in multiple linear regression geochemical mixing models, G^3 (Geochemistry, Geophysics, Geosystems), 16, 4021-4027, doi:10.1002/2015GC006132.

Hall, R., 2002. Cenozoic geological and plate tectonic evolution of SE Asia and the SW Pacific: Computer-based reconstructions, model and animations, Journal of Asian Earth Sciences, 20, 353–431.

Hall, R., 2012. Late Jurassic–Cenozoic reconstructions of the Indonesian region and the Indian Ocean, Tectonophysics, 570–571, 1–41.

Kano, K., Kato, H., Yanagisawa, Y., and Yoshida, F., 1991. Stratigraphy and geologic history of the Cenozoic of Japan, Reports, Geological Survey of Japan, 274, 114.

Kimura, J.-I., Stern, R.J., and Yoshida, T., 2005. Reinitiation of subduction and magmatic responses in SW Japan during Neogene time, Geological Society of America Bulletin, 117, 969–986.

Kimura, J-I., Nagahashi, Y., Satoguchi, Y., Chang, Q., 2015. Origins of felsic magmas in Japanese subduction zone: Geochemical characterizations of tephra from caldera-

forming eruptions <5 Ma. Geochemistry, Geophysics, Geosystems, doi:10.1002/2015GC005854

Kutterolf, S., Schindlbeck, J.C., Scudder, R.P., Freundt, A., Pickering, K.T., Labanieh, S., Heydolph, K., Murray, R.W., Saito, S., Naruse, H., Underwood, M.B., and Wu, H., 2014. Large volume submarine ignimbrites in the Shikoku Basin: An example for explosive volcanism in the Western Pacific during the late Miocene. Geochemistry, Geophysics, Geosystems, 15(5): 1837–1851, doi:10.1002/2014GC005263.

Machida, H., 1999. The stratigraphy, chronology and distribution of distal marker-tephras in and around Japan. Global and Planetary Change, 21: 71-94.

Machida, H., 2002. Volcanoes and tephras in the Japan area. Global Environmental Research, 6(2): 19-28.

Machida, H. and Arai, F., 2003. Atlas of tephra in and around Japan. Univ. of Tokyo Press, 336p.

Mahony, S.H., Wallace, L.M., Miyoshi, M., Villamor, P., Sparks, R.S.J., Hasenaka, T., 2011. Volcano-tectonic interactions during rapid plate-boundary evolution in the Kyushu region, SW Japan. Geological Society of America Bulletin, 123, 2201-2223.

Pickering, K. T., Underwood, M.B., Saito, S., Naruse, H., Kutterolf, S., Scudder, R.P., Park, J.-O., Moore, G. F., and Slagle, A., 2013. Depositional architecture, provenance, and tectonic/eustatic modulation of Miocene submarine fans in the Shikoku Basin: Results from Nankai Trough Seismogenic Zone Experiment. Geochemistry, Geophysics, Geosystems, 14(6): 1722–1739, doi:10.1002/ggge.20107.

Saitoh, Y., Ishikawa, T., Tanimizu, M., Murayama, M., Ujiie, Y., Yamamoto, Y., Ujiie, K., Kanamatsu, T., 2015. Sr, Nd, and Pb isotope compositions of hemipelagic sediment in the Shikoku Basin: Implications for sediment transport by the Kuroshio and Philippine Sea plate motion in the late Cenozoic. Earth and Planetary Science Letters, 421, 47-57, doi:10.1016/j.epsl.2015.04.001

Sato, H., 1994. The relationship between late Cenozoic tectonic events and stress field and basin development in northeast Japan, Journal of Geophysical Research, 99:B11, 22261–22274

Schindlbeck, J.C., Kutterolf, S., Freundt, A., Scudder, R.P., and Pickering, K.T., 2013. Emplacement processes of submarine volcaniclastic deposits (IODP Site C0011, Nankai Trough). Marine Geology. 343: 115-124.

Sdrolias, M., Roest, W.R., and Müller, R.D., 2004. An expression of Philippine Sea plate rotation: The Parece Vela and Shikoku Basins, *Tectonophysics*, **394**, 69–86.

Shinjo R., and Kato Y., 2000, Geochemical constraints on the origin of bimodal magmatism at the Okinawa Trough, an incipient back-arc basin: Lithos, v. 54 p. 117-137.

Soh, W., Pickering, K.T., Taira, A., and Tokuyiama, H., 1991. Basin evolution in the arc-arc Izu Collision Zone, Mio-Pliocene Miura Group, central Japan, Journal of the Geological Society of London, 148, 317–330.

Stern, R.J., Fouch, M.J., Klemperer, S.L., 2003. An overview of the Izu–Bonin–Mariana subduction factory,in: J. Eiler (Ed.), Inside the Subduction Factory, Geophysical Monograph, vol. 138, Am. Geophys. Un (2003), pp. 175–222.

Sugimoto T., Shibata T., Yoshikawa M., Takemura K., 2006, Sr-Nd-Pb isotopic and major and trace element compositions of the Yufu-Tsurumi volcanic rocks: Implications for the magma genesis of the Yufu-Tsurumi volcanoes, northeast Kyushu, Japan: Journal of Mineralogical and Petrological Sciences, v. 101, p. 270–275.

Suzuki, K., and Tatsumi, Y., 2006. Re–Os systematics of high-Mg andesites and basalts from the Setouchi volcanic belt, SW Japan: implications for interaction between wedge mantle and slab-derived melt. Geochemical Journal, 40, 297–307

Taira, A., 2001. Tectonic evolution of the Japanese island arc system, Annual Review of Earth and Planetary Sciences, 29,109–134.

Tamura, Y., and Tatsumi, Y., 2002. Remelting of an andesitic crust as a possible origin for rhyolitic magma in oceanic arcs: an example from the Izu–Bonin arc. Journal of Petrology 43:1029-1047.

Tamura, Y. et al., 2010. Missing Oligocene crust of the Izu-Bonin Arc: Consumed or rejuvenated during collision?, Journal of Petrology, 51, 823–846.

Tani, K., Dunkley, D.J.. Kimua, J.-L., Wysoczanski, R.J., Yamada, K., and Tatsumi, Y., 2010. Syncollisional rapid granitic magma formation in an arc-arc collision zone: Evidence from the Tanzawa plutonic complex, Japan, *Geology*, **38**, 215–218.

Taylor, B., 1992. Rifting and the volcanic-tectonic evolution of the Izu-Bonin-Mariana arc, in Proc. ODP, Sci. Results, edited by B. Taylor, et al., 126, 627–651, ODP, College Station, TX.

Taylor, R.T., and Nesbitt, R.W., 1998, Isotopic characteristics of subduction fluids in an intra-oceanic setting, Izu-Bonin Arc: Japan. Earth and Planetary Science Letters, v. 164 n. 1-2, p. 79-98.

Taylor, S.R. and McLennan, S.M., 1985, The continental crust: Its composition and evolution. Blackwell Scientific Pub., 328 pp.

Yamaji A., 1990. Rapid intra-arc rifting in Miocene northeast Japan. Tectonics, 9:365–78

Yamamoto, T., 2009. Sedimentary processes caused by felsic caldera-forming volcanism in the Late Miocene to Early Pliocene intra-arc Aizu basin, NE Japan arc, in: K. Nemeth, V. Manville, K. Kano (Eds.), Source to sink: from volcanic eruptions to volcaniclastic deposits on the Pacific Rim. Sedimentary Geology, 220, 337–348

Yamazaki, T., Yakahashi, M., Iryu, Y., Sato, T., Oda, M., Takayanagi, H., Chiyonobu, S., Nishimura, A., and Ooka, T., 2010. Philippine Sea Plate motion since the Eocene estimated from paleomagnetism of seafloor drill cores and gravity cores, Earth and Planetary Science Letters, 62, 495–502.